ORGANOMETALLICS Article
Cite This: Organometallics XXXX, XXX, XXX−XXX
pubs.acs.org/Organometallics

Syntheses, Crystal Structures, and Photoluminescence of a Series of Iridium(III) Complexes Containing the Pentafluorosulfanyl Group

Xiao-Feng Ma,[†] Xu-Feng Luo,[†] Zhi-Ping Yan, Zheng-Guang Wu,* Yue Zhao,* You-Xuan Zheng,* and Jing-Lin Zuo*

State Key Laboratory of Coordination Chemistry, Jiangsu Key Laboratory of Advanced Organic Materials, School of Chemistry and Chemical Engineering, Nanjing University, Nanjing 210093, People's Republic of China

Supporting Information

ABSTRACT: Eight neutral iridium(III) complexes (**Ir1**−**Ir8**) containing an electron-withdrawing pentafluorosulfanyl ($-SF_5$) group on cyclometalated ligands with different ancillary ligands were synthesized and investigated. 2-(3/4-(Pentafluorosulfanyl)phenyl)-pyrimidine (for **Ir1** and **Ir2**), 1-(3/4-(pentafluorosulfanyl)phenyl)isoquinoline (for **Ir3** and **Ir4**), and 2-(3/4-(pentafluorosulfanyl)phenyl)pyridine (for **Ir5**−**Ir8**) were chosen as cyclometalated ligands and 2,2,6,6-tetramethylheptane-3,5-dione (for **Ir1**−**Ir4**), tetraphenylimidodiphosphinate (for **Ir5** and **Ir6**), and bis(diphenylphorothioyl)amide (for **Ir7** and **Ir8**) were used as ancillary ligands. The crystal structures of **Ir1**, **Ir3**, **Ir4**, **Ir6**, and **Ir8** also confirmed the identities of these complexes. Complexes **Ir1**, **Ir2**, and **Ir5**−**Ir8** exhibit sky blue to green emissions (480−533 nm) with high photoluminescence quantum efficiency yields up to 94.7% in CH_2Cl_2 solution at room temperature. Complexes **Ir3** and **Ir4** are red phosphors (λ_{max} = 607 nm, Φ = 76.8% for **Ir3** and λ_{max} = 627 nm, Φ = 49.2% for **Ir4**, respectively). Theoretical calculations were carried out to provide a further study of the orbital distributions and electronic states of eight Ir(III) complexes. Additionally, ion detection studies reveal that **Ir2** has the potential for detecting Hg^{2+} ion.

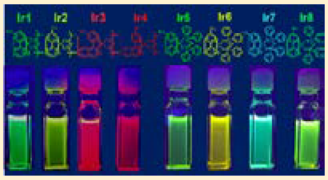

INTRODUCTION

Over the years, octahedral d^6 iridium(III) complexes have attracted much attention. The strong spin−orbit coupling (SOC) caused by the central Ir(III) atom can promote the triplet to ground state radiative transition, leading to high phosphorescence quantum yields at room temperature. This unique character makes Ir(III) complexes promising candidates for applications in organic light-emitting devices,[1] organic light-emitting electrochemical transistors,[2] low-power upconversion,[3] photocatalysts,[4] luminescent biological labeling,[5] nonlinear optics,[6] and ion detection.[7]

For neutral heteroleptic Ir(III) complexes $Ir(C^\wedge N)_2LX$, the cyclometalated ligands C^N are usually 2-phenylpyridine derivatives. According to previous reports, moieties with electron-withdrawing/-donating properties, such as −F, $-CF_3$ (trifluoromethyl), and −OMe (methoxyl) groups, were introduced into the ligands to influence the HOMO and LUMO energy band gaps and adjust the photophysical properties of the Ir(III) complexes.[8] Pentafluorosulfanyl ($-SF_5$) is considered as a "super-trifluoromethyl" group because $-SF_5$ has the peculiarity of fluorine beyond the $-CF_3$ group.[9] Furthermore, $-SF_5$ is a very strong electron-withdrawing group (EWG) with bulky, chemically inert, polar, and hydrophobic properties. Since $-CF_3$ has been extensively applied to Ir(III) complexes in recent years, it can be expected that $-SF_5$ also has great application potential in similar materials. In 2015, Shavaleev et al. introduced $-SF_5$ into cationic Ir(III) complexes,[10] and in 2018, a theoretical study of these cationic Ir(III) complexes was performed by Junquera-Hernández et al. In 2017, Pal et al. investigated the properties of two neutral **R1** and **R2** complexes containing $-SF_5$ groups (Scheme 1).[11] However, the reported Ir(III) complexes with $-SF_5$ units are still rare.

Inspired by the work of Pal et al., we introduced pyrimidyl or isoquinolyl to replace pyridyl in the cyclometalated ligands of 2-(3/4-(pentafluorosulfanyl)phenyl)pyrimidine (3/4-pmd) and 1-(3/4-(pentafluorosulfanyl)phenyl)isoquinoline (3/4-piq), and the four complexes **Ir1**−**Ir4** were obtained with tetramethylheptane-3,5-dione (tma) as an ancillary ligand (Scheme 1). The nitrogen heterocycles of the cyclometalated ligands can influence the electronic states and change the photophysical properties of the phosphors to give green and red emissions. To exploit more diverse molecular structures, tetraphenyl imidodiphosphinate (tpip) and bis-(diphenylphorothioyl)amide (stpip) ancillary ligands were further introduced, which were developed by our group previously.[12] Herein, 2-(3/4-(pentafluorosulfanyl)phenyl)-pyridine (3/4-ppy) species were chosen as representatives of cyclometalated ligands and the four complexes **Ir5**−**Ir8** were obtained (Scheme 2). The coordination capability of oxygen/sulfur atoms with an iridium atom is strong, resulting in high reaction yields. In addition, the ancillary ligand tpip/stpip with a bulky group could suppress the accumulation of molecules, which is helpful for reducing triplet−triplet annihilation (TTA) and achieving a high photoluminescence quantum yield (PLQY).[13] These eight complexes show sky blue, green, and red emissions peaking from 480 to 627 nm, with high

Received: June 11, 2019

DOI: 10.1021/acs.organomet.9b00392
Organometallics XXXX, XXX, XXX−XXX

Scheme 1. Synthetic Routes of Complexes Ir1−Ir4 and the Chemical Structures of Reference Complexes R1−R3

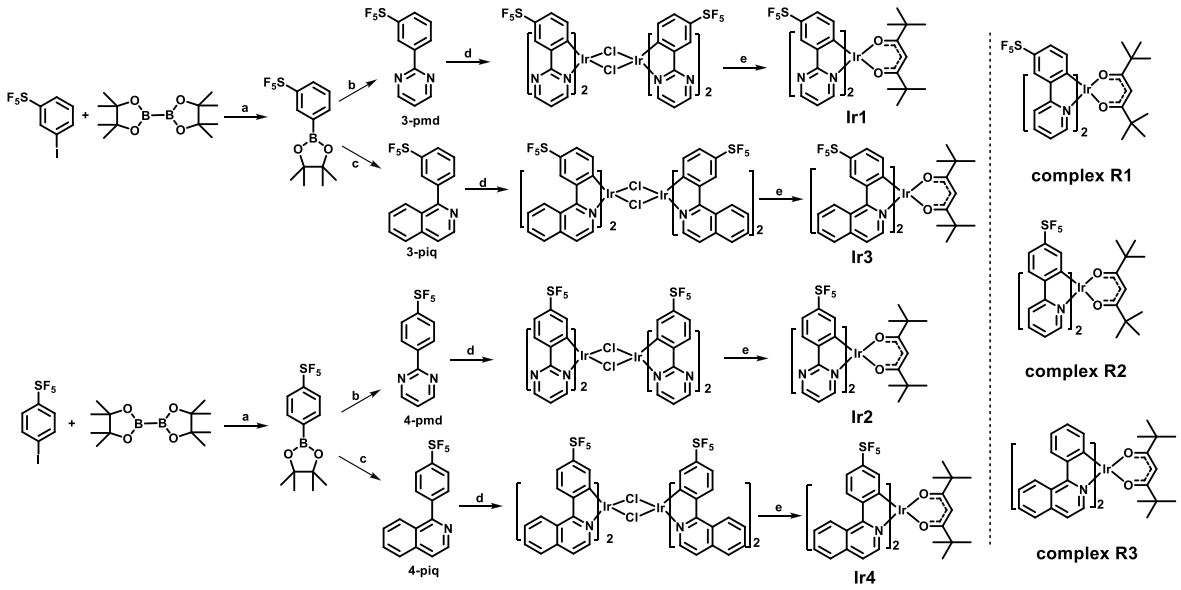

Scheme 2. Synthetic Routes of Complexes Ir5−Ir8

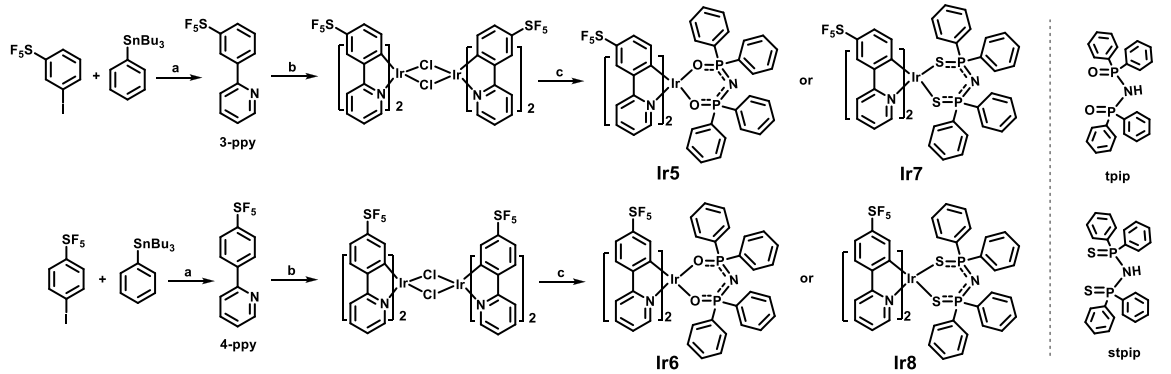

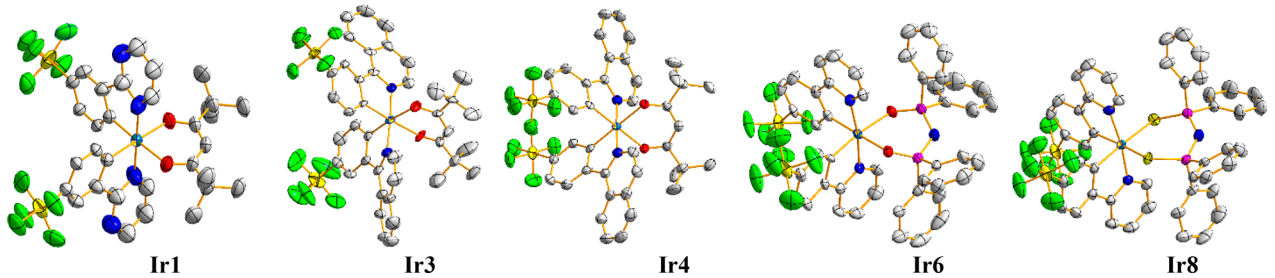

Figure 1. ORTEP diagrams of **Ir1** (CCDC 1900417), **Ir3** (CCDC 1900416), **Ir4** (CCDC 1900418), **Ir6** (CCDC 1900420), and **Ir8** (CCDC 1900419). Hydrogen atoms are omitted for clarity.

PLQYs up to 94.7%. Furthermore, taking **Ir2** as an example, we also explored its application possibility in ion detection, and the preliminary results show that it has the potential to be used as a probe for detecting Hg^{2+}.

■ RESULTS AND DISCUSSION

Preparation and Characterization of Compounds. The cyclometalated ligands 3/4-pmd and 3/4-piq were synthesized using a Suzuki coupling reaction, and 3/4-ppy ligands were synthesized using a Stille coupling reaction (Schemes 1 and 2). Eight complexes were prepared by the reaction of their corresponding chloride-bridged dimmers with tma, tpip, and stpip, respectively. All products were characterized by HRMS spectrometry, and **Ir1**, **Ir2**, and **Ir5**−**Ir7** were characterized by ^{1}H, ^{13}C, and ^{19}F NMR spectrometry, but there is a lack of NMR spectra for **Ir3**, **Ir4**, and **Ir8** due to their poor solubility. In addition, the crystal structures of **Ir1**, **Ir3**, **Ir4**, **Ir6**, and **Ir8** further confirmed the identities of these complexes.

All single crystals were obtained by vacuum sublimation, and the crystal diagrams of **Ir1**, **Ir3**, **Ir4**, **Ir6**, and **Ir8** are displayed in Figure 1; the corresponding crystallographic data are given in Tables S1 and S2. As can be seen clearly from the structural diagrams of the crystals, the iridium atom is surrounded by C,

DOI: 10.1021/acs.organomet.9b00392
Organometallics XXXX, XXX, XXX−XXX

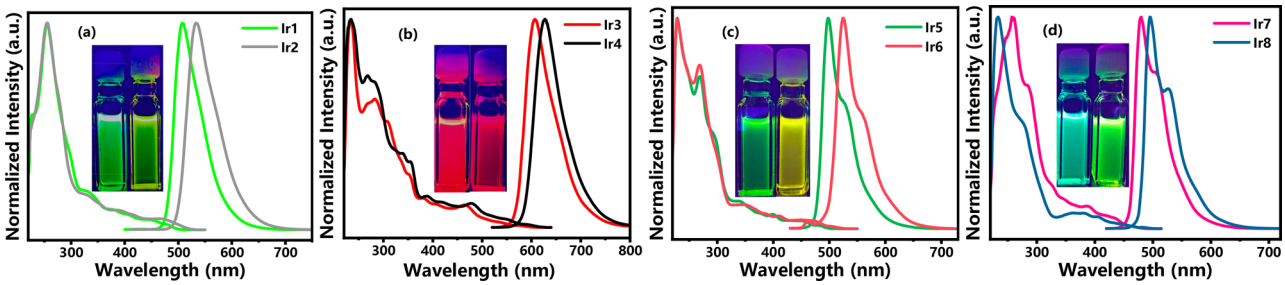

Figure 2. UV−vis absorption and emission spectra of complexes (a) **Ir1** and **Ir2**, (b) **Ir3** and **Ir4**, (c) **Ir5** and **Ir6**, and (d) **Ir7** and **Ir8** in degassed CH_2Cl_2 (5×10^{-5} mol L^{-1}) at room temperature.

Table 1. Photophysical Properties of Complexes Ir1−Ir8

complex	λ_{abs}[a] (nm)	λ_{em}[a] (nm)	CIE (*x*, *y*)	Φ[b] (%)	τ_p[a] (μs)
Ir1	256/332/451	507	(0.23, 0.63)	98	1.62
Ir2	255.5/329/390/471	533	(0.36, 0.62)	89	1.81
Ir3	234.5/283/308/465	607	(0.64, 0.36)	80	2.10
Ir4	234/268/355/389/477.5	627	(0.68, 0.32)	51	1.87
Ir5	229/269/340/400	498/527	(0.20, 0.60)	86	1.61
Ir6	228.5/268.5/349/411	525/558	(0.32, 0.63)	90	2.04
Ir7	257.5/283.5/386/434	480/506	(0.15, 0.42)	69	1.66
Ir8	233.5/275/378/405	495/526	(0.22, 0.60)	66	1.68

[a]Measured in degassed CH_2Cl_2 solution at a concentration of 5×10^{-5} mol L^{-1} at room temperature. [b]Measured in degassed CH_2Cl_2 solution at a concentration of 5×10^{-5} mol L^{-1} at room temperature and using *fac*-Ir(ppy)$_3$ as the standard sample (Φ = 97%).

N, and S/O atoms from cyclometalated ligands and ancillary ligands, and the crystals exhibit a twisted-octahedral coordination geometry. For **Ir1**, **Ir3**, **Ir4**, and **Ir6**, the [O−Ir−O] angles are in the range of 88.0(5)−89.80(14)°, and for **Ir8**, the [S−Ir−S] angle is 102.26(3)°. The [C−Ir−N] angles of the five complexes range from 79.84(15) to 98.10(2)°. The Ir−C, Ir−N, and Ir−O bond lengths are in the ranges of 1.960(6)−2.022(4), 1.946(16)−2.062(3), and 2.113(10)−2.221(4) Å, respectively. In addition, the Ir−S bond lengths are in the range of 2.4636(9)−2.4825(10) Å, a bit longer than that of Ir−O bonds. These results are reasonable, since they are similar to the parameters of the reported Ir(III) complex.[14]

The thermal properties of eight complexes were characterized by thermogravimetric analysis (TGA, Figure S1). All compounds exhibit good thermal stability, and the decomposition temperatures corresponding to 5% weight loss on heating during TGA are in the range of 278−393 °C.

Photophysical Properties. The UV−vis absorption and photoluminescence (PL) spectra of eight complexes measured in degassed CH_2Cl_2 (5×10^{-5} mol L^{-1}) are shown in Figure 2, and their photophysical data are collected in Table 1. All absorption spectra show broad and intense bands below 320 nm, assigned to the spin-allowed intraligand ^{1}LC (π−π^*) transitions of the cyclometalated ligands and ancillary ligands. The weak bands up to 520 nm can be assigned to spin-allowed metal to ligand charge-transfer bands (^{1}MLCT), partially overlapped by the broad LC absorptions, and spin-forbidden ^{3}MLCT transition bands caused by the large SOC, which was introduced by the iridium center and is a prerequisite for phosphorescent emission.[15] The absorption profiles of each group of complexes are similar, indicating similar electronic and vibrational structures of the ground states (S_0) and the first excited states (S_1).

The strongest emission peaks of **Ir1**−**Ir4** at 507, 533, 607, and 627 nm, respectively, are produced by the electronic transitions between the lowest triplet excited state and ground state (^{1}MLCT and ^{3}MLCT). Emission peaks of **Ir5**−**Ir8** at 498, 525, 480, and 495 nm with shoulder peaks at 527, 558, 506, and 526 nm, respectively, are produced by MLCT and LC. The CIE color coordinates of **Ir1** and **Ir2** are (0.23, 0.63) and (0.36, 0.62) with green emissions, those of **Ir3** and **Ir4** are (0.64, 0.36) and (0.68, 0.32) with red emissions, and those of **Ir5**−**Ir8** are (0.21, 0.60), (0.32, 0.63), (0.15, 0.42), and (0.22, 0.60) with sky blue to green emissions, respectively. Furthermore, all complexes show high quantum yields in the range of 51−98%.

In addition, the PL spectra of complexes **R1** and **R2** were also investigated as references under the same conditions, which are shown in Figure S2. **R1** and **R2** are green phosphors peaking at 502 and 532 nm, respectively. When **Ir1**/**Ir2** and **Ir3**/**Ir4** are compared with **R1**/**R2**, it can be found that the newly introduced pyrimidyl unit on the cyclometalated ligand has a small influence on PL spectra, while the isoquinolyl moiety causes a significant red shift. For **Ir5**/**Ir6**, there is a slight red shift when the ancillary ligand tma is replaced by tpip. However, there are obvious 22 and 37 nm blue shifts for **Ir7** and **Ir8**, respectively, when tma is replaced by stpip.

It also can be seen that there are approximately 15−26 nm differences in emission wavelengths for each group of Ir(III) complexes with similar cyclometalated ligands and the same ancillary ligand in Figure 2, indicating that the position of the $-SF_5$ group on the cyclometalated ligand affects the emission properties of the complexes. These differences are due to the increasing electron-withdrawing nature of the $-SF_5$ group when it is moved from a meta position to a para position with respect to the Ir−C bond of the cyclometalated ligand, thus leading to an obvious blue shift. Furthermore, the emission spectrum of **Ir2** at 77 K was investigated as an example (Figure S3). It can be found that at 77 K one peak splits into two peaks with an unobvious band, which is due to lowering of the π−π^* excited state (or destabilization of the MLCT excited state) on the formation of rigid media at low temperature.[16]

DOI: 10.1021/acs.organomet.9b00392
Organometallics XXXX, XXX, XXX−XXX

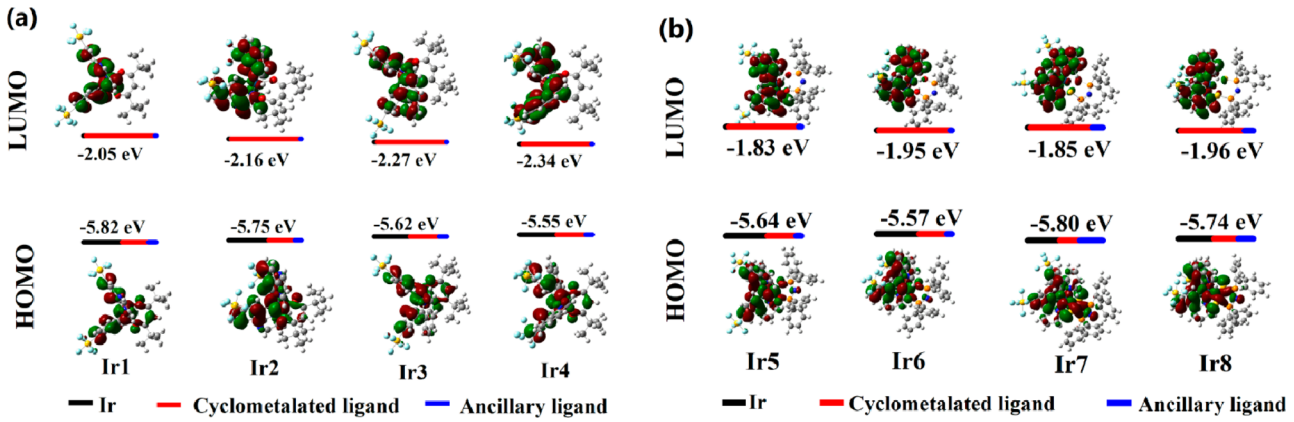

Figure 3. DFT calculated HOMO/LUMO energy levels of complexes **Ir1**−**Ir8** and the percentage compositions of iridium atom (black line), cyclometalated ligand (red line), and ancillary ligand (blue line).

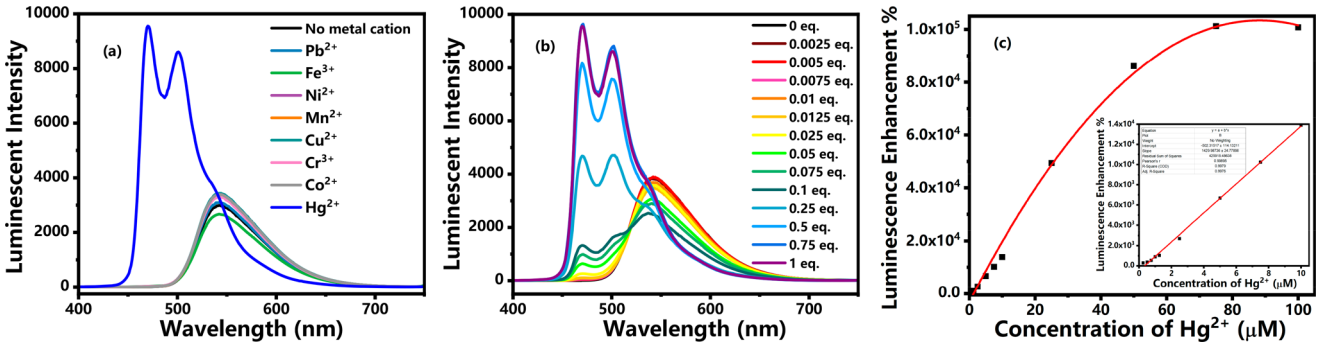

Figure 4. (a) Luminescence spectra of **Ir2** (1×10^{-4} mol L^{-1}) in the presence of various metal cations (1 equiv) in CH_3CN/H_2O (4/1, v/v) solution. (b) Changes in the luminescence spectra of **Ir2** (1×10^{-4} mol L^{-1}) in CH_3CN/H_2O (4/1, v/v) solutions with various amounts of Hg^{2+} ions (0−1 equiv). (c) Corresponding luminescence enhancement at 470 nm with an increase in the Hg^{2+} concentrations.

The phosphorescence lifetimes (τ_p) of the eight complexes are in the range of 1.43−1.79 μs in degassed CH_2Cl_2 solutions at room temperature and are indicative of the phosphorescence origins from triplet metal to ligand charge transfer (^{3}MLCT) and/or triplet ligand to ligand charge transfer (^{3}LLCT) states. The specific results are shown in Figure S4.

Theoretical Calculations. It is well understood that photophysical properties of the Ir(III) complexes are strongly dependent on the characters of their frontier orbitals and the resulting HOMO and/or LUMO energy gaps. To provide further study of the electronic states and the orbital distributions of eight complexes, theoretical calculations were performed on optimized geometries in CH_2Cl_2.[17] Contour plots of FMOs are shown in Figure 3. The energies and percentage compositions of ligands and metal orbitals are given in Table S3.

From Figure 3 it can be seen that the LUMOs of the eight Ir(III) complexes mostly distribute over the π^* orbitals of the cyclometalated ligands (81.42−95.56%) and to a small extent on d orbitals of the iridium atom (3.20−4.72%) and ancillary ligands (1.17−14.33%). The HOMO orbitals are mostly located on the cyclometalated ligands (26.54−40.30%) together with d orbitals of the iridium atom (42.80−56.24%) with a small portion on the ancillary ligands (6.94−20.56%). A larger scale distribution of electron clouds on the iridium atom indicates the efficient MLCT of the phosphorescent complexes, crucial to the high PL quantum efficiencies. In addition, incorporation of the $-SF_5$ EWG on the cyclometalated phenyl ring helps to stabilize the frontier molecular orbitals, leading to a blue shift in the observed emission color for complexes. Taking **Ir3** and **Ir4** as examples, there are 23 and 3 nm blue shifts in comparison with reference complex **R3**, which has a similar molecular structure except for the $-SF_5$ unit, reported by Tian et al. in 2010.[18] What is more, according to the results of **Ir5**−**Ir8** it can be seen that the HOMO/LUMO contributions of stpip in **Ir7**/**Ir8** are more than that of tpip in **Ir5**/**Ir6** and larger band gaps also cause obvious blue shifts. The calculation results indicate that the introduction of nitrogen heterocycles on the cyclometalated ligand and tpip/stpip on the ancillary ligand affects the orbital distributions and HOMO/LUMO levels of the Ir(III) complexes. Thus, the photophysical properties of Ir(III) complexes can be tuned through controlled functionalization of both the cyclometalated and ancillary ligands.

Tentative Exploration of Ion Detection. As mentioned before, chemical structures of cyclometalated ligands can strongly affect the photophysical properties of Ir(III) complexes. When the cyclometalated ligands contain specific metal-coordinating elements, there is a good chance that the presence of metal ions can lead to dramatic changes in the photophysical properties of complexes.[19] Herein, the heterocyclic **Ir2** was chosen as an example to explore if it could be used as a highly selective sensor for Hg^{2+} ion.

For an excellent chemosensor, high selectivity is a matter of necessity.[20] Herein, a selective experiment was carried out by luminescent spectra with different metal ions. As shown in Figure 4a, in a solution of CH_3CN/H_2O (4/1, v/v), **Ir2** exhibits a maximum emission peak at 543 nm. After the

DOI: 10.1021/acs.organomet.9b00392
Organometallics XXXX, XXX, XXX−XXX

addition of 1 equiv of Hg^{2+}, **Ir2** shows a prominent emission change, whereas very weak variations were observed upon addition of an equal amount of other metal ions, such as Fe^{3+}, Ni^{2+}, Mn^{2+}, Cu^{2+}, Cr^{3+}, and Co^{2+}. Therefore, **Ir2** displays a high selectivity in detecting Hg^{2+}.

The response of **Ir2** to various amounts of Hg^{2+} ions (0−1 equiv) was further investigated, and the results are shown in Figure 4b. After 0.0025 equiv of Hg^{2+} was added, a new emission peak at 470 nm appeared, and with an increase in Hg^{2+} ratios, one emission peak splits up into three peaks. Upon addition of 1 equiv of Hg^{2+}, **Ir2** exhibits a blue shift of 73 nm with the strongest emission peak at 470 nm, corresponding to an evident change in emission color from yellow to blue. Hence, **Ir2** shows efficient colorimetric sensing of Hg^{2+}. The corresponding luminescence enhancement is shown in Figure 4c. According to the IUPAC definition, the calculated detection limit is down to 4 ppb.[21] These observations indicate that **Ir2** has the potential to serve as a probe for detecting Hg^{2+} ions. On comparison of **Ir2** with other Ir(III)-based Hg^{2+} sensors,[22] it can be found that **Ir2** exhibits not only an apparent response but also visual color changes upon the addition of Hg^{2+}. It shows high selectivity for Hg^{2+} with naked-eye detection, and the detection limit is down to 4 ppm (20 nM), lower than that for most other Ir(III)-based Hg^{2+} sensors.

To explain the significant change of emission after the addition of Hg^{2+}, the emission spectra of 4-pmd and 4-pmd-Hg^{2+} in CH_3CN/H_2O (4/1, v/v) were further investigated (Figure S5). Obviously, in comparison to the newly formed emission band (470 nm) of the binding product, free ligand emission exhibits a blue shift of 65 nm. After 1.0 equiv of Hg^{2+} ions was added, the emission of the ligand was observed with a new maximum peak at 498 nm, which may be caused by the coordination of the Hg^{2+} ion and 4-pmd ligand. Then, the complexes **Ir9** and **Ir10** with 2-(4-(pentafluorosulfanyl)-phenyl)pyridine and 2-(4-trifluorophenyl)pyridine as the main ligands and 2,2,6,6-tetramethylheptane-3,5-dione as the ancillary ligand were investigated under the same test conditions, respectively (Figures S6 and S7). Unexpectedly, after addition of various amounts of Hg^{2+} ions (0−1 equiv), the luminescence spectra of **Ir9** and **Ir10** were similar to that of **Ir2** in CH_3CN/H_2O (4/1, v/v) solution (Figure 4b). This means that the cause of changes in emission spectra is not the bonding between the Hg^{2+} ion and nitrogen in the pyrimidine unit or S atom in the pentafluorosulfanyl group, but the decomposition of the complex, which was proved in some former publications by Mei et al.[23] and the Li group.[24] After the addition of Hg^{2+} ion, the tmd ancillary ligand is dissociated from the complex, while the MeCN is inserted to form the $[Ir(4\text{-pmd})_2(MeCN)_2]^+\cdot NO_3^-$ complex. Additionally, the emission lifetime of the **Ir2**−Hg^{2+} adduct at 470 nm was also measured as 69.79 ns (Figure S8), different from that of **Ir2**. This indicated that the coordination of MeCN reduced the lifetime greatly. The interaction among Hg^{2+}, MeCN, and **Ir2** was responsible for the significant variation in optical signals.

■ CONCLUSIONS

In summary, eight Ir(III) complexes bearing strongly electron withdrawing pentafluorosulfanyl groups on the cyclometalated ligands were synthesized. 2-(3/4-(Pentafluorosulfanyl)-phenyl)pyrimidine, 1-(3/4-(pentafluorosulfanyl)phenyl)-isoquinoline, and 2-(3/4-(pentafluorosulfanyl)phenyl)pyridine were chosen as cyclometalated ligands, and 2,2,6,6-tetramethylheptane-3,5-dione, tetraphenylimidodiphosphinate, and bis(diphenylphorothioyl)amide were used as ancillary ligands. The crystal structures of **Ir1**, **Ir3**, **Ir4**, **Ir6**, and **Ir8** further confirmed their identity. These complexes display sky blue, green, and red emissions with photoluminescence quantum efficiency yields ranging from 49.2% to 94.7%. Theoretical calculations provide further study of the electronic states and the orbital distribution of the complexes. What is more, tentative exploration results show **Ir2** has great potential to serve as a probe for detecting Hg^{2+} ion.

■ EXPERIMENTAL SECTION

The ligands 3/4-ppy and tpip/stpip and Ir(III) chloro-bridged dimers were synthesized according to previous reports.[10−12]

Syntheses of 3/4-pmd and 3/4-piq. 3/4-Iodophenylsulfur pentafluoride (1.8 mmol), bis(pinacolato)diboron (2.7 mmol), KOAc (9.0 mmol), and $PdCl_2$(dppf) (0.09 mmol) were added to 14 mL of dehydrated 1,4-dioxane in a 50 mL sealed-tube bottle. The mixture was heated at 100 °C overnight, poured into water, and extracted with CH_2Cl_2. Then, the obtained oil was placed in a 25 mL sealed-tube bottle with 2-bromopyrimidine or 1-chloroisoquinoline (1.0 mmol), Na_2CO_3 (3.0 mmol), and $Pd(PPh_3)_4$ (0.04 mmol) and heated at 75 °C in THF and H_2O (3/1, v/v) overnight. After cooling, the mixture was extracted with CH_2Cl_2 and purified by column chromatography to give 3/4-pmd or 3/4-piq.

Syntheses of Iridium(III) Complexes. A mixture of $IrCl_3$ (1 mmol) and different main ligands (3/4-pmd or 3/4-piq, 2.5 mmol) in 2-ethoxyethanol and water (20 mL, 3/1, v/v) was refluxed for 24 h. After cooling, the solid precipitate was filtered to give the crude cyclometalated Ir(III) chloro-bridged dimer. The corresponding chloro-bridged dimer (0.5 mmol) and ancillary ligand salt (1.1 mmol) in 2-ethoxyethanol (20 mL) were refluxed for 24 h. The 2-ethoxyethanol was evaporated, and water was added. Then, the mixture was extracted with CH_2Cl_2 and chromatographed, giving complexes **Ir1**−**Ir8**, which were further purified by vacuum sublimation. The ^{1}H NMR, ^{13}C NMR, and ^{19}F NMR spectra are given in Figures S9−S16, and their mass spectra are shown in Figures S18−S25.

Ir1. Yellow solid with 52% yield. ^{1}H NMR (400 MHz, $CDCl_3$): δ 8.84 (dd, J = 4.7, 2.2 Hz, 2H), 8.50 (dd, J = 5.7, 2.2 Hz, 2H), 8.36 (d, J = 2.5 Hz, 2H), 7.22 (dd, J = 5.6, 4.9 Hz, 2H), 7.15 (dd, J = 8.5, 2.5 Hz, 2H), 6.45 (d, J = 8.5 Hz, 2H), 5.58 (s, 1H), 0.92 (s, 18H). ^{13}C NMR (100 MHz, $CDCl_3$): δ 195.07, 167.55, 159.03, 146.45, 140.24, 137.16, 133.69, 131.16, 128.70, 127.54, 126.16, 125.92 (m), 125.76, 125.20 (m), 120.70, 89.93, 41.14, 28.02. ^{19}F NMR (376 MHz, $CDCl_3$): δ 86.90 (p, J = 160 Hz, 2F), 63.90 (d, J = 160 Hz, 10F). MS (HR ESI): m/z calcd for $C_{31}H_{31}F_{10}IrN_4O_2S_2$ $[M + H]^+$ 939.1436, found 939.1407.

Ir2. Yellow solid with 54% yield. ^{1}H NMR (400 MHz, $CDCl_3$): δ 8.84 (dd, J = 4.7, 2.2 Hz, 2H), 8.50 (dd, J = 5.7, 2.2 Hz, 2H), 8.05 (d, J = 8.6 Hz, 2H), 7.33 (dd, J = 8.6, 2.2 Hz, 2H), 7.25−7.21 (m, 2H), 6.61 (d, J = 2.1 Hz, 2H), 5.56 (s, 1H), 0.90 (s, 18H). ^{13}C NMR (100 MHz, $CDCl_3$): δ 194.97, 152.64, 140.17, 137.10, 131.11, 129.71, 128.78, 128.42, 127.50, 126.53, 126.02, 121.07, 117.88, 89.90, 41.14, 28.01. ^{19}F NMR (376 MHz, $CDCl_3$): δ 85.93 (p, J = 160 Hz, 2F), 62.57 (d, J = 160 Hz, 8F). MS (HR ESI): m/z calcd for $C_{31}H_{31}F_{10}IrN_4O_2S_2$ $[M + H]^+$ 939.1436, found 939.1433.

Ir3. Red solid with 50% yield. ^{19}F NMR (376 MHz, $CDCl_3$): δ 87.94 (p, J = 160 Hz, 2F), 64.18 (d, J = 160 Hz, 8F). MS (HR ESI): m/z calcd for $C_{41}H_{37}F_{10}IrN_2O_2S_2$ $[M + H]^+$ 1037.1844, found 1037.1827.

Ir4. Red solid with 50% yield. ^{19}F NMR (376 MHz, $CDCl_3$): δ 86.23 (p, J = 160 Hz, 2F), 62.56 (d, J = 160 Hz, 8F). MS (HR ESI): m/z calcd for $C_{41}H_{37}F_{10}IrN_2O_2S_2$ $[M + Na]^+$ 1059.1664, found 1059.1714.

Ir5. Yellow solid with 88% yield. ^{1}H NMR (400 MHz, $CDCl_3$): δ 9.02 (d, J = 5.5 Hz, 2H), 7.83 (d, J = 2.4 Hz, 2H), 7.78−7.68 (m, 6H), 7.50 (td, J = 7.9, 1.4 Hz, 2H), 7.32 (tt, J = 4.0, 3.0 Hz, 10H),

DOI: 10.1021/acs.organomet.9b00392
Organometallics XXXX, XXX, XXX−XXX

7.15 (td, J = 7.5, 1.2 Hz, 2H), 7.01−6.94 (m, 6H), 6.73−6.67 (m, 2H), 6.16 (d, J = 8.5 Hz, 2H). ^{13}C NMR (101 MHz, $CDCl_3$): δ 166.40, 150.70, 149.57, 148.68, 148.51, 145.27, 139.93, 139.87, 139.63, 138.56, 138.51, 138.34, 137.29, 132.26, 130.85, 130.79, 130.74, 130.55, 130.50, 130.44, 130.23, 129.68, 128.05, 127.99, 127.92, 127.61, 127.54, 127.48, 125.50 (t), 122.06, 120.15 (t), 118.20. ^{19}F NMR (376 MHz, $CDCl_3$): δ 87.74 (p, J = 160 Hz, 2F), 64.14 (d, J = 160 Hz, 8F). MS (HR ESI): m/z calcd for $C_{46}H_{34}F_{10}IrN_3O_2P_2S_2$ $[M + H]^+$ 1170.1115, found 1170.1104.

Ir6. Yellow solid with 83% yield. ^{1}H NMR (400 MHz, $CDCl_3$): δ 9.01 (d, J = 5.0 Hz, 2H), 7.76 (ddd, J = 12.3, 7.6, 1.6 Hz, 4H), 7.70 (d, J = 8.0 Hz, 2H), 7.56−7.47 (m, 4H), 7.38−7.27 (m, 10H), 7.21 (dd, J = 8.5, 2.3 Hz, 2H), 7.15−7.09 (m, 2H), 6.94 (td, J = 7.7, 3.0 Hz, 4H), 6.75−6.69 (m, 2H), 6.28 (d, J = 2.2 Hz, 2H). ^{19}F NMR (376 MHz, $CDCl_3$): δ 86.56 (p, J = 160 Hz, 2F), 62.58 (d, J = 160 Hz, 8F). MS (HR ESI): m/z calcd for $C_{46}H_{34}F_{10}IrN_3O_2P_2S_2$ $[M + H]^+$ 1170.1115, found 1170.1101.

Ir7. Yellow solid with 81% yield. ^{1}H NMR (400 MHz, CD_2Cl_2): δ 9.16 (dd, J = 5.9, 1.0 Hz, 2H), 7.98−7.88 (m, 4H), 7.84 (d, J = 2.4 Hz, 2H), 7.72 (d, J = 7.8 Hz, 2H), 7.53−7.43 (m, 6H), 7.37−7.30 (m, 6H), 7.22−7.16 (m, 2H), 7.01−6.92 (m, 6H), 6.37 (ddd, J = 7.4, 5.9, 1.4 Hz, 2H), 5.97 (d, J = 8.5 Hz, 2H). ^{13}C NMR (101 MHz, CD_2Cl_2): δ 165.99, 158.35, 151.24, 149.25, 149.09, 144.79, 141.09, 141.02, 140.60, 139.97, 139.90, 139.59, 137.27, 131.00, 130.88, 130.73, 130.40, 130.11, 130.00, 128.75, 128.62, 126.11, 123.10, 120.97, 119.31. ^{19}F NMR (376 MHz, CD_2Cl_2): δ 86.89 (p, J = 160 Hz, 2F), 63.77 (d, J = 160 Hz, 8F). MS (HR ESI): m/z calcd for $C_{46}H_{34}F_{10}IrN_3P_2S_4$ $[M + H]^+$ 1202.0659, found 1202.0705.

Ir8. Yellow solid with 85% yield. ^{19}F NMR (376 MHz, $CDCl_3$): δ 86.24 (p, J = 160 Hz, 2F), 62.67 (d, J = 160 Hz, 8F). MS (HR ESI): m/z calcd for $C_{46}H_{34}F_{10}IrN_3P_2S_4$ $[M + H]^+$ 1202.0659, found 1202.1717.

■ ASSOCIATED CONTENT

Supporting Information

The Supporting Information is available free of charge on the ACS Publications website at DOI: 10.1021/acs.organomet.9b00392.

Crystallographic data, details of the calculations, and characterization data (PDF)

Accession Codes

CCDC 1900416−1900420 contain the supplementary crystallographic data for this paper. These data can be obtained free of charge via www.ccdc.cam.ac.uk/data_request/cif, or by emailing data_request@ccdc.cam.ac.uk, or by contacting The Cambridge Crystallographic Data Centre, 12 Union Road, Cambridge CB2 1EZ, UK; fax: +44 1223 336033.

■ AUTHOR INFORMATION

Corresponding Authors

*E-mail for Z.-G.W.: wuzhengguang_zy@163.com.
*E-mail for Y.Z.: zhaoyue@nju.edu.cn.
*E-mail for Y.-X.Z.: yxzheng@nju.edu.cn.
*E-mail for J.-L.Z.: zuojl@nju.edu.cn.

ORCID

Yue Zhao: 0000-0001-6094-4087
You-Xuan Zheng: 0000-0002-1795-2492
Jing-Lin Zuo: 0000-0003-1219-8926

Author Contributions

†X.-F.M. and X.-F.L. contributed equally to this paper.

Notes

The authors declare no competing financial interest.

■ ACKNOWLEDGMENTS

This study was supported by the National Natural Science Foundation of China (51773088, 21975119).

■ REFERENCES

(1) (a) Su, S. J.; Cai, C.; Kido, J. RGB Phosphorescent Organic Light-Emitting Diodes by Using Host Materials with Heterocyclic Cores: Effect of Nitrogen Atom Orientations. *Chem. Mater.* **2011**, *23*, 274−284. (b) Su, S. J.; Chiba, T.; Takeda, T.; Kido, J. Pyridine-Containing Triphenylbenzene Derivatives with High Electron Mobility for Highly Efficient Phosphorescent OLEDs. *Adv. Mater.* **2008**, *20*, 2125−2130. (c) Bettington, S.; Tavasli, M.; Bryce, M. R.; Beeby, A.; Al-Attar, H.; Monkman, A. P. Tris-Cyclometalated Iridium(III) Complexes of Carbazole(fluorenyl)pyridine Ligands: Synthesis, Redox and Photophysical Properties, and Electrophosphorescent Light-Emitting Diodes. *Chem. - Eur. J.* **2007**, *13*, 1423−1431.

(2) Zhou, Y.; Han, S. T.; Zhou, G. J.; Wong, W. Y.; Roy, V. A. L. Ambipolar Organic Light-Emitting Electrochemical Transistor Based on a Heteroleptic Charged Iridium(III) Complex. *Appl. Phys. Lett.* **2013**, *102*, 083301.

(3) Zhao, W.; Castellano, F. N. Upconverted Emission from Pyrene and Di-tert-butylpyrene Using $Ir(ppy)_3$ as Triplet Sensitizer. *J. Phys. Chem. A* **2006**, *110*, 11440−11445.

(4) Belmore, K. A.; Vanderpool, R. A.; Tsai, J.-C.; Khan, M. A.; Nicholas, K. M. Transition-Metal-Mediated Photochemical Disproportionation of Carbon Dioxide. *J. Am. Chem. Soc.* **1988**, *110*, 2004−2005.

(5) Lo, K. K. Luminescent Rhenium(I) and Iridium(III) Polypyridine Complexes as Biological Probes, Imaging Reagents, and Photocytotoxic Agents. *Acc. Chem. Res.* **2015**, *48*, 2985−2995.

(6) Liu, R.; Dandu, N.; McCleese, C.; Li, Y.; Lu, T.; Li, H.; Yost, D.; Wang, C.; Kilina, S.; Burda, C.; Sun, W. Influence of a Naphthaldiimide Substituent at the Diimine Ligand on the Photophysics and Reverse Saturable Absorption of Pt^{II} Diimine Complexes and Cationic Ir^{III} Complexes. *Eur. J. Inorg. Chem.* **2015**, *2015*, 5241−5253.

(7) Hou, L.; Shangguan, M.; Lu, Z.; Yi, S.; Jiang, X.; Jiang, H. A Cyclometalated Iridium(III) Complex-Based Fluorescence Probe for Hypochlorite Detection and its Application by Test Strips. *Anal. Biochem.* **2019**, *566*, 27−31.

(8) (a) Kim, J. H.; Kim, S. Y.; Cho, D. W.; Son, H. J.; Kang, S. O. Influence of Bulky Substituents on the Photophysical Properties of Homoleptic Iridium(III) Complexes. *Phys. Chem. Chem. Phys.* **2019**, *21*, 6908−6916. (b) Sajoto, T.; Djurovich, P. I.; Tamayo, A.; Yousufuddin, M.; Bau, R.; Thompson, M. E.; Holmes, R. J.; Forrest, S. R. Blue and Near-UV Phosphorescence from Iridium Complexes with Cyclometalated Pyrazolyl or N-Heterocyclic Carbene Ligands. *Inorg. Chem.* **2005**, *44*, 7992−8003.

(9) Umemoto, T.; Garrick, L. M.; Saito, N. Discovery of Practical Production Processes for Arylsulfur Pentafluorides and Their Higher Homologs, Bis- and Tris-(Sulfur Pentafluorides): Beginning of a New Era of Super-Trifluoromethyl Arene Chemistry and Its Industry. *Beilstein J. Org. Chem.* **2012**, *8*, 461−471.

(10) (a) Shavaleev, N. M.; Xie, G. H.; Varghese, S.; Cordes, D. B.; Slawin, A. M. Z.; Momblona, C.; Ortí, E.; Bolink, H. J.; Samuel, I. D. W.; Zysman-Colman, E. Green Phosphorescence and Electroluminescence of Sulfur Pentafluoride-Functionalized Cationic Iridium(III) Complexes. *Inorg. Chem.* **2015**, *54*, 5907−5914. (b) Junquera-Hernández, J. M.; Escobar, J.; Ortí, E. Electronic Nature of the Emitting Triplet in SF_5-Substituted Cationic Ir(III) Complexes. *Polyhedron* **2018**, *140*, 1−8.

(11) Pal, A. K.; Henwood, A. F.; Cordes, D. B.; Slawin, A. M. Z.; Samuel, I. D. W.; Zysman-Colman, E. Blue-to-Green Emitting Neutral Ir(III) Complexes Bearing Pentafluorosulfanyl Groups: A Combined Experimental and Theoretical Study. *Inorg. Chem.* **2017**, *56*, 7533−7544.

(12) (a) Zhu, Y. C.; Zhou, L.; Li, H. Y.; Xu, Q. L.; Teng, M. Y.; Zheng, Y. X.; Zuo, J. L.; Zhang, H. J.; You, X. Z. Highly Efficient

DOI: 10.1021/acs.organomet.9b00392
Organometallics XXXX, XXX, XXX−XXX

Green and Blue-Green Phosphorescent OLEDs Based on Iridium Complexes with the Tetraphenylimidodiphosphinate Ligand. *Adv. Mater.* **2011**, *23*, 4041−4046. (b) Xia, J. C.; Liang, X.; Yan, Z. P.; Wu, Z. G.; Zhao, Y.; Zheng, Y. X.; Zhang, W. W. Iridium(III) Phosphors with Bis(diphenylphorothioyl)amide Ligand for Efficient Green and Sky-Blue OLEDs with EQE of Nearly 28%. *J. Mater. Chem. C* **2018**, *6*, 9010−9016.

(13) Lee, J.; Chopra, N.; Eom, S.-H.; Zheng, Y.; Xue, J.; So, F.; Shi, J. Effects of Triplet Energies and Transporting Properties of Carrier Transporting Materials on Blue Phosphorescent Organic Light Emitting Devices. *Appl. Phys. Lett.* **2008**, *93*, 123306.

(14) (a) Wright, S. E.; Richardson-Solorzano, S.; Stewart, T. N.; Miller, C. D.; Morris, K. C.; Daley, C. J. A.; Clark, T. B. Accessing Ambiphilic Phosphine Boronates through C-H Borylation by an Unforeseen Cationic Iridium Complex. *Angew. Chem., Int. Ed.* **2019**, *58*, 2834−2838. (b) Traskovskis, K.; Kokars, V.; Belyakov, S.; Lesina, N.; Mihailovs, I.; Vembris, A. Emission Enhancement by Intramolecular Stacking between Heteroleptic Iridium(III) Complex and Flexibly Bridged Aromatic Pendant Group. *Inorg. Chem.* **2019**, *58*, 4214−4222. (c) Lai, P. N.; Teets, T. S. Ancillary Ligand Effects on Red-Emitting Cyclometalated Iridium Complexes. *Chem. - Eur. J.* **2019**, *25*, 6026−6037. (d) Na, H.; Cañada, L. M.; Wen, Z.; Wu, J. I.; Teets, T. S. Mixed-Carbene Cyclometalated Iridium Complexes with Saturated Blue Luminescence. *Chem. Sci.* **2019**, *10*, 6254−6260. (e) Lai, P. N.; Brysacz, C. H.; Alam, M. K.; Ayoub, N. A.; Gray, T. G.; Bao, J.; Teets, T. S. Highly Efficient Red-Emitting Bis-Cyclometalated Iridium Complexes. *J. Am. Chem. Soc.* **2018**, *140*, 10198−10207.

(15) (a) Zanoni, K. P. S.; Vilela, R. R. C.; Silva, I. D. A.; Iha, N. Y. M.; Eckert, H.; de Camargo, A. S. S. Photophysical Properties of Ir(III) Complexes Immobilized in MCM-41 via Templated Synthesis. *Inorg. Chem.* **2019**, *58*, 4962−4971. (b) Cortes-Arriagada, D.; Sanhueza, L.; Gonzalez, I.; Dreyse, P.; Toro-Labbe, A. About the Electronic and Photophysical Properties of Iridium(III)-Pyrazino[2,3-*f*][1,10]-Phenanthroline Based Complexes for Use in Electroluminescent Devices. *Phys. Chem. Chem. Phys.* **2016**, *18*, 726−734.

(16) Colombo, M. G.; Brunold, T. C.; Riedener, T.; Giide, H. U. Facial Tris Cyclometalated Rhodium^{3+} and Iridium^{3+} Complexes: Their Synthesis, Structure, and Optical Spectroscopic Properties. *Inorg. Chem.* **1994**, *33*, 545−550.

(17) Frisch, M. J.; Trucks, G. W.; Schlegel, H. B.; Scuseria, G. E.; Robb, M. A.; Cheeseman, J. R.; Scalmani, G.; Barone, V.; Mennucci, B.; Petersson, G. A.; Nakatsuji, H.; Caricato, M.; Li, X.; Hratchian, H. P.; Izmaylov, A. F.; Bloino, J.; Zheng, G.; Sonnenberg, J. L.; Hada, M.; Ehara, M.; Toyota, K.; Fukuda, R.; Hasegawa, J.; Ishida, M.; Nakajima, T.; Honda, Y.; Kitao, O.; Nakai, H.; Vreven, T.; Montgomery, J. A., Jr.; Peralta, J. E.; Ogliaro, M. B. F.; Heyd, J. J.; Brothers, E.; Kudin, K. N.; Staroverov, V. N.; Kobayashi, R.; Normand, J.; Raghavachari, K.; Rendell, A.; Burant, J. C.; Iyengar, S. S.; Tomasi, J.; Cossi, M.; Rega, N.; Millam, J. M.; Klene, M.; Knox, J. E.; Cross, J. B.; Bakken, V.; Adamo, C.; Jaramillo, J.; Gomperts, R.; Stratmann, R. E.; Yazyev, O.; Austin, A. J.; Cammi, R.; Pomelli, C.; Ochterski, J. W.; Martin, R. L.; Morokuma, K.; Zakrzewski, V. G.; Voth, G. A.; Salvador, P.; Dannenberg, J. J.; Dapprich, S.; Daniels, A. D.; Farkas, O.; Foresman, J. B.; Ortiz, J. V.; Cioslowski, J.; Fox, D. J. *Gaussian 09, Revision A*; Gaussian, Inc.: Wallingford, CT, 2009.

(18) Tian, N.; Lenkeit, D.; Pelz, S.; Fischer, L. H.; Escudero, D.; Schiewek, R.; Klink, D.; Schmitz, O. J.; González, L.; Schäferling, M.; Holder, E. Structure-Property Relationship of Red- and Green-Emitting Iridium(III) Complexes with Respect to Their Temperature and Oxygen Sensitivity. *Eur. J. Inorg. Chem.* **2010**, *2010*, 4875−4885.

(19) (a) Georgiev, N. I.; Krasteva, P. V.; Bojinov, V. B. A Ratiometric 4-Amido-1,8-Naphthalimide Fluorescent Probe Based on Excimer-Monomer Emission for Determination of pH and Water Content in Organic Solvents. *J. Lumin.* **2019**, *212*, 271−278. (b) Ribes, À.; Aznar, E.; Santiago-Felipe, S.; Xifre-Perez, E.; Tormo-Mas, M. À.; Pemán, J.; Marsal, L. F.; Martínez-Máñez, R. Selective and Sensitive Probe Based in Oligonucleotide-Capped Nanoporous Alumina for the Rapid Screening of Infection Produced by Candida Albicans. *ACS Sens* **2019**, *4*, 1291−1298. (c) Lu, H.; Zhang, S. S.; Liu, H. Z.; Wang, Y. W.; Shen, Z.; Liu, C. G.; You, X. Z. Experimentation and Theoretic Calculation of a BODIPY Sensor Based on Photo-induced Electron Transfer for Ions Detection. *J. Phys. Chem. A* **2009**, *113*, 14081−14086.

(20) (a) Erdemir, S.; Kocyigit, O. A Novel Dye Based on Phenolphthalein-Fluorescein as a Fluorescent Probe for the Dual-Channel Detection of Hg^{2+} and Zn^{2+}. *Dyes Pigm.* **2017**, *145*, 72−79. (b) Zhao, Q.; Cao, T.; Li, F.; Li, X.; Jing, H.; Yi, T.; Huang, C. A Highly Selective and Multisignaling Optical-Electrochemical Sensor for Hg^{2+} Based on a Phosphorescent Iridium(III) Complex. *Organometallics* **2007**, *26*, 2077−2081.

(21) Peng, L.; Zhao, Q. D.; Wang, D. J.; Zhai, J. L.; Wang, P.; Pang, S.; Xie, T. F. Ultraviolet-Assisted Gas Sensing: A Potential Formaldehyde Detection Approach at Room Temperature Based on Zinc Oxide Nanorods. *Sens. Actuators, B* **2009**, *136*, 80−85.

(22) (a) Lu, F. N.; Yamamura, M.; Nabeshima, T. A Highly Selective and Sensitive Ratiometric Chemodosimeter for Hg^{2+} Ions Based on an Iridium(III) Complex via Thioacetal Deprotection Reaction. *Dalton Trans* **2013**, *42*, 12093−12100. (b) Tong, B. H.; Zhang, M.; Han, Z.; Mei, Q. B.; Zhang, Q. F. Novel Colorimetric Phosphorescent Chemodosimeter for Hg^{2+} Based Iridium(III) Complex with Phosphonodithioate Auxiliary Ligand. *J. Organomet. Chem.* **2013**, *724*, 180−185.

(23) Mei, Q. B.; Guo, Y. H.; Tong, B. H.; Weng, J. N.; Zhang, B.; Huang, W. Phosphorescent Chemosensor for Hg^{2+} and Acetonitrile Based on Iridium(III) Complex. *Analyst* **2012**, *137*, 5398−5402.

(24) Wu, Y. Q.; Jing, H.; Dong, Z. S.; Zhao, Q.; Wu, H. Z.; Li, F. Y. Ratiometric Phosphorescence Imaging of Hg(II) in Living Cells Based on a Neutral Iridium(III) Complex. *Inorg. Chem.* **2011**, *50*, 7412−7420.

DOI: 10.1021/acs.organomet.9b00392
Organometallics XXXX, XXX, XXX−XXX